Annals of Glaciology

Article

Cite this article: Voveris J, Serreze M (2023). A tale of two events: Arctic rain-on-snow meteorological drivers. *Annals of Glaciology* 1–12. https://doi.org/10.1017/aog.2023.25

Received: 29 September 2022
Revised: 26 January 2023
Accepted: 3 March 2023

Keywords:
Atmosphere/ice/ocean interactions; climate change; ice/atmosphere interactions

Corresponding author:
Jessica Voveris;
E-mail: jessica.voveris@colorado.edu

A tale of two events: Arctic rain-on-snow meteorological drivers

Jessica Voveris and Mark Serreze

National Snow and Ice Data Center, Cooperative Institute for Research in Environmental Sciences, University of Colorado, Boulder, USA

Abstract

Arctic rain-on-snow (ROS) events can have significant impacts on Arctic wildlife and socio-economic systems. This study addresses the meteorology of two different Arctic ROS events. The first, occurring near Nuuk, Greenland, generated significant impacts, including slush avalanches. The second, less severe, event occurred within the community of Iqaluit, Nunavut, Canada. This research utilizes atmospheric reanalysis, automated surface observation station data and atmospheric soundings to determine the meteorological conditions driving these events and the differences between each case. In both cases, atmospheric blocking played a leading role in ROS initiation, with atmospheric rivers – narrow bands of high water vapor transport, typically originating from the tropics and subtropics – having both direct and indirect effects. Cyclone-induced low-level jets and resultant 'warm noses' of higher air temperatures and moisture transport were other key features in ROS generation. To our knowledge, our study is the first to visualize how the varying strength and manifestation of these coupled features contribute to differences in the severity of Arctic ROS events. The meteorological drivers identified here find support from other studies on Arctic ROS events and are similar to weather features associated with Arctic precipitation events of extreme magnitude.

Introduction

Characterizing rain-on-snow events and their impacts

Arctic rain-on-snow (ROS) events occur when liquid precipitation, in the form of rain or freezing rain, falls on an existing snowpack (Grenfell and Putkonen, 2008; Rennert and others, 2009; Bieniek and others, 2018; Serreze and others, 2021). In general, research on Alaskan ROS events noted that these conditions are most likely to occur from October through April – with some studies narrowing it further to November through March – when conditions are favorable and a snowpack is present (Bieniek and others, 2018; Pan and others, 2018; Crawford and others, 2020). North American and Eurasian ROS events may also occur during this seasonal window (Cohen and others, 2015).

ROS events in the middle latitudes have been studied extensively, including how their occurrence relates to geographic position relative to sources of maritime moisture or the number of rain days a location may experience (Kattelmann, 1997; McCabe and others, 2007; Cohen and others, 2014; Garvelmann and others, 2015). Impacts from flooding are well known, with the combination of heavy rainfall and melting of the underlying snowpack (McCabe and others, 2007). An area may be more susceptible to ROS-generated flooding due to several factors: rain over a large catchment area (which leads to a high amount of run-off), the potential for additional snowmelt conditions and changes in snow cover dynamics (snow metamorphism) and elevated rainfall over extended periods (when storm systems should be producing snow) (Kattelmann, 1997; Singh and others, 1997; Garvelmann and others, 2015; Guan and others, 2016).

ROS events can disrupt ground transportation and aviation operations, and wet-snow (or slush) avalanches resulting from ROS can damage infrastructure (Putkonen and Roe, 2003; Hansen and others, 2014). Officials may close roads and airports due to ice formation, isolating Arctic communities (Hansen and others, 2014). As a notable example of infrastructure impacts, a slush avalanche in Longyearbyen (Svalbard) destroyed a pedestrian bridge, and major roads that serviced the community had to be closed for several days (Hansen and others, 2014). The authors add that Arctic locations are susceptible to wet-snow avalanches in a warming climate, as current infrastructure was not originally built with these natural disasters in mind.

Following ROS occurrence, the ice layers that accumulate on, or within, the snowpack act as barriers to foraging, sometimes leading to mass starvation of caribou, reindeer and musk oxen (Rennert and others, 2009; Forbes and others, 2016; Serreze and others, 2021). Ice formation may also force animals to seek other sources of food further away from their regular environments, exacerbating the conditions leading to starvation (Serreze and others, 2021). Examples include an Arctic ROS event that occurred on Banks Island in Canada during October of 2003 that led to the demise of an estimated 20 000 musk oxen, an event in Svalbard in January of 2012 – which produced one of the largest numbers of reindeer carcasses found in the following summer – and an event in the Yamal Peninsula in northern Russia during the autumn of 2013

https://doi.org/10.1017/aog.2023.25 Published online by Cambridge University Press

that starved ~61 000 reindeer (out of a total of 275 000) (Rennert and others, 2009; Hansen and others, 2014; Serreze and others, 2015; Forbes and others, 2016).

Known meteorology concerning Arctic rain-on-snow events

Generally, near-surface air temperatures in the region of an Arctic ROS event increase dramatically preceding the onset of precipitation, typically over a relatively short time period (Rennert and others, 2009; Hansen and others, 2014; Serreze and others, 2021). This causes rain to fall during part of the event (or throughout the entirety of the event) and may cause additional surface melting. Air temperatures then decrease following the event, often to well below freezing (Serreze and others, 2021). Liquid water freezes and forms a thick glaze of ice along the surface of the snow layer or within the snowpack (Serreze and others, 2021).

This sequence of shifting temperatures frequently involves an advancing extratropical cyclone (which generates the initial precipitation), with a cold front then progressing through the area (Rennert and others, 2009). Working in tandem with the overall precipitation event, increased warm air advection with these systems causes additional melting of the surface snow layer through amplified mixing and turbulent fluxes (Semmens and others, 2013). For example, Rennert and others (2009) described a strong anticyclonic ridge at the synoptic scale that initially developed over the Banks Island region preceding the October 2003 ROS event. This feature led to strong, southwesterly flow bringing warmer, moister air into the area. Lift (upward motion), triggered by an approaching shortwave trough (extratropical cyclone), initiated precipitation across the region. The precipitation first began as snow then transitioned to rain as air temperatures rose (Rennert and others, 2009).

Some studies noted ROS connections with atmospheric blocking and atmospheric rivers (ARs). Crawford and others (2020) described a link between blocking patterns and ROS conditions in Alaska, in which a strong pressure gradient builds between a ridge of high-pressure and an approaching extratropical storm system. This gradient instigates further warm air advection and transport of positive anomalies in precipitable water, the total atmospheric water vapor contained within an atmospheric column. Serreze and others (2015) associated an AR with the January 2012 Svalbard ROS event, which coincided with an extreme event in total precipitation. Studies for the middle latitudes documented links between ROS events in mountainous regions in the inland Western US and landfalling ARs along the US West Coast (Guan and others, 2016; Trubilowicz and Moore, 2017). Nevertheless, it is widely acknowledged that additional research is needed to understand the weather patterns influencing Arctic ROS events and how features like ARs and blocking setups impact their formation (Rennert and others, 2009; Bieniek and others, 2018).

Research questions posed for this study

The Arctic Rain-on-Snow Study, a team of interdisciplinary researchers and part of the National Science Foundation's Navigating the New Arctic initiative, focuses on better understanding Arctic ROS events and their impacts on Arctic communities. One of the project goals is to assess the meteorological conditions most influential in setting up ROS occurrences. As mentioned, Arctic ROS events occur at times of the year (October through April) when precipitation should usually be falling as snow and during which solar radiation is limited or even absent, depending on the latitude. This implies a key role of warm (and moist) air advection and transport from lower latitudes. As the Arctic continues to warm, one can expect both the seasonality and intensity of ROS events to change. This prompts three questions:

(1) What are the primary meteorological conditions at varying spatial scales linked to Arctic ROS occurrence?
(2) Do synoptic scale blocking patterns and ARs play important roles in Arctic ROS initiation?
(3) Are the strength and presence of these features (and others) influential in the severity of ROS impacts?

Case study selection, data sources and methodology

Selection of case studies

We selected two divergent ROS events for this study. The first event occurred in Western Greenland in mid-April of 2016. A team of researchers confirmed it by investigating wet-snow avalanches near Nuuk, Greenland, using remote-sensing data (Abermann and others, 2019). The authors concluded that over 800 wet-snow avalanches initiated during this ROS event and documented that an automated surface observation station was destroyed on 11 April. This coincided with the day of highest air temperatures and precipitation rates.

Abermann and others (2019) briefly examined the associated weather conditions. A high-pressure system built over the region beginning on 9 April 2016. It continued to strengthen, progressing through April 10. As a warm front approached southwestern Greenland, air temperatures increased rapidly, and this feature provided additional moisture advection needed to produce significant precipitation. Abermann and others (2019) documented that the Greenland Ecosystem Monitoring Program's automated meteorological station near Nuuk, Greenland, recorded this rapid warming (an increase of 22.2°C from 9 to 11 April) and a precipitation total of 25 mm during this same 2 d period. An additional station with the Asiaq monitoring network for Nuuk recorded a slightly smaller temperature increase of 14.6°C but a larger precipitation total of 49 mm for the 2 d period, being a location closer to the maritime environment.

The second event occurred on 19 January 2021, in Iqaluit (Nunavut, Canada), confirmed by an eyewitness report on social media and relayed to the Arctic Rain-on-Snow Study team by one of its members. This case presented an opportunity to research a ROS event that had not been studied previously. In the lead up to this event, much of Canada had experienced a swing from seasonally cold to above normal air temperatures during the early part of January 2021. Around the beginning of the new year, atmospheric reanalysis data indicated surface air temperature anomalies of −5 to −20°C across much of the Canadian Arctic. By the second week in January, atmospheric reanalysis showed the flip to +5 to +20°C surface air temperature anomalies over the same area, likely due to the combination of a building ridge of high-pressure over western Canada and a blocking feature over eastern Canada.

According to an article published for the Nunatsiaq News on 18 January 2021, and posted on the Local Environmental Observer Network (a web-based platform built for community sharing of unusual weather events), Iqaluit was expected to continue experiencing unseasonably high air temperatures through the middle of the month. A low-pressure system was projected to move into the area through the coming week, bringing warm air from the south, and allowing air temperatures to remain around the freezing mark (Nunatsiaq News, 2021). This was likely the same system that produced ROS conditions on 19 January. Climate data provided by the Government of Canada reported that the snow depth at Iqaluit was 25 cm (9.84 inches) on 6 January 2021. There was a period of missing data from

https://doi.org/10.1017/aog.2023.25 Published online by Cambridge University Press

7 January through 19 January, but the next observation for Iqaluit on 20 January indicated a snow depth of 25 cm. Therefore, we can safely assume that there was a snowpack at the time rain was reported on 19 January.

Documented impacts related to ROS for the 2021 Iqaluit event were very limited. However, the effects resulting from the increased air temperatures, including on the day of the event, were noted. Iqaluit broke its maximum air temperature record for 19 January, with a new record of 0.5°C (CBC News, 2021). According to the article from CBC News, the new temperature record broke the previous record of −2.2°C, set in 1958. Subsequently, the differences in impacts resulting from ROS during these two events allow us to compare the meteorological features linked to ROS occurrence and the difference in strength of these features that led to these varying impacts.

Data types and acquisition

We use ERA5 reanalysis output from the European Centre for Medium-Range Weather Forecasts (ECMWF) for this study. ERA5, like other reanalysis datasets, is a combination of observational and modeling datasets and performs well in its depiction of meteorological variables in comparison to direct observations, including temperature, specific humidity and wind speed (Graham and others, 2019). However, relative to its predecessor, ERA-Interim, ERA5 advances the discernment of synoptic- and meso-scale features, which includes cyclones, a key precipitation forcing for these two ROS events. Comparisons of radiosonde and PILOT data (an alternative upper-air balloon observation) prior to data assimilation shows an improved fit for tropospheric temperature, winds and humidity (Hoffmann and others, 2019; Hersbach and others, 2020). Another key finding from the Hoffmann and others (2019) effort demonstrates that ERA5 trajectories (based within Lagrangian transport models) better conserve stratospheric-level potential temperature, leading to smaller data assimilation increments that improve the uniformity of ECMWF's forecast model and observations. ERA5 also produces hourly output at a 31 km horizontal resolution, higher than ERA-Interim's 80 km resolution (Hersbach and others, 2020).

We access ERA5 data from the 1979 to present dataset. ERA5 data are available hourly, and we selected the 00Z (UTC) and 12Z files for this study. These times coincide with upper-air launch times (radiosondes), and 12 h increments still provide sufficient temporal resolution to examine the synoptic makeup of ROS events. An application program interface allows for different meteorological parameters to be downloaded to data files.

We supplement this study with direct observations, including automated surface observation stations and atmospheric sounding data (radiosondes). The observation network across the Arctic remains sparse, with many of these automated sites restricted to airports. Other limitations include intermittent outages and upper-air data only being provided twice a day. Sounding data utilized with this study presents a unique dataset not analyzed in previous Arctic ROS studies. We obtained sounding data for Aasiaat, Greenland (north of Nuuk), and for Iqaluit from the University of Wyoming sounding archive using python code provided by MetPy, a program developed by the University Corporation for Atmospheric Research. Automated station data for Godthaab (Nuuk) and Iqaluit were available from the Iowa Environmental Mesonet surface observation archive from Iowa State University (https://mesonet.agron.iastate.edu/ASOS/).

Data visualization methodology

We created data visualizations of ERA5 reanalysis using select python programming modules. Visualizations were divided into three atmospheric heights: upper levels, middle levels and lower levels. Weather variables were chosen at these levels to best characterize various meteorological processes. Figure 1 provides an overview of the meteorological variables used in each analysis and at each atmospheric level. Additionally, MetPy code (noted above) was deployed in building skew-ts, commonly used to visualize sounding data. A separate python-based program was written to provide time series data visualizations of the surface station observations. We created these time series graphs to show the progression of temperature and dewpoint temperature changes and precipitation type transitions, including during each ROS event.

Results

April 2016 Western Greenland rain-on-snow event

Atmospheric reanalysis

As introduced earlier, the April 2016 Western Greenland ROS event generated numerous wet-snow avalanches near Nuuk (Abermann and others, 2019). Several meteorological features

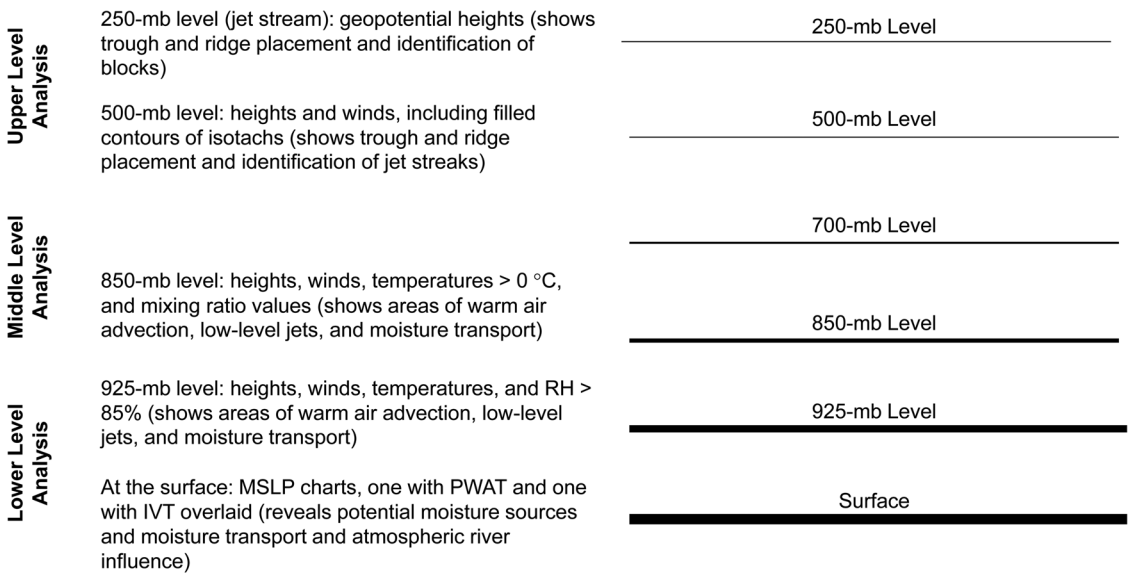

Figure 1. Weather variables examined with the reanalysis data.

https://doi.org/10.1017/aog.2023.25 Published online by Cambridge University Press

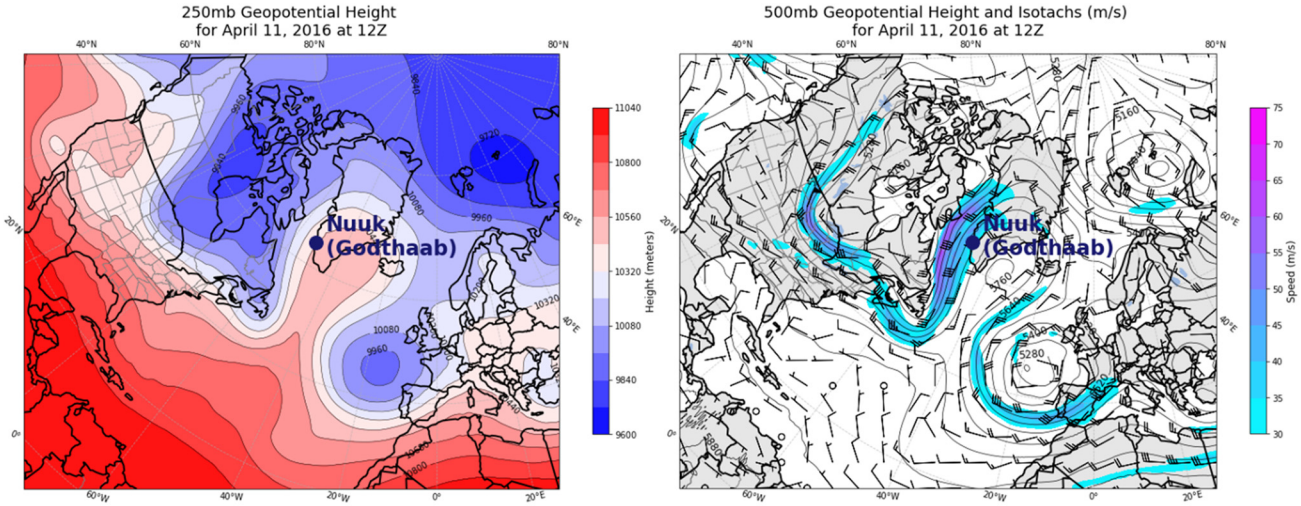

Figure 2. The 2016 Western Greenland case upper atmospheric levels. The 250 mb geopotential heights are plotted on the left, and the 500 mb heights and winds are plotted on the right. The 500 mb panel also includes isotachs (lines of constant wind speed) in m s^{-1} in filled contours, in addition to wind barbs that indicate both direction and speed.

stand out in the ERA5 data. In the upper levels (Fig. 2), an Omega Block is prominent at both the jet stream level (250 mb level) and the 500 mb level. An Omega Block resembles a capital Greek letter Omega through the shape of the tropospheric, synoptic scale waveform. In this case, the ridge extending across Greenland is sandwiched between a broad trough across eastern Canada and a cutoff low over western Europe. It represents a block because of the predominant meridional flow and the persistent disruption to the general west-to-east progression of weather systems.

Strong wind speeds (above 50 m s^{-1} over Baffin Bay) are present at the 500 mb level along the gradient between the ridge over southern Greenland and the broad trough over eastern Canada. This area of higher wind speeds represents a jet streak. The location of interest – in this case Nuuk (Godthaab), Greenland – falls within this area that would likely be experiencing greater precipitation rates due to the additional jet dynamics. In addition, these winds are predominantly out of the south on the left (western) side of the ridge, as seen in the flag direction of the wind barbs in the 500 mb analysis. This implies a warmer air mass moving into the region. An opposing northerly flow follows on the right (eastern) side of the ridge, which likely assisted in maintaining the block.

Precipitation associated with this event can be linked to the approaching shortwave trough extending over much of the province of Quebec (Fig. 2). ERA5 reanalysis fields show dynamically induced rising motion on 11 April 2016, coinciding with precipitation over much of the area near Nuuk. Nuuk lies within a fjord, with surrounding terrain approaching 1000 m. While suggesting that orographic lifting contributed to the elevated precipitation amounts, our interpretation is that dynamic lift was the dominant precipitation forcing.

In the atmospheric mid- to low-levels, strong moisture transport and warm air advection accompany a cyclone-induced low-level jet (Fig. 3). These features are usually associated with the pre-cold frontal sector of an extratropical cyclone (Ralph and others, 2005). They can be important factors in determining what locations experience precipitation and how much of it. The cited study also notes that 'the low-level jet is an integral part of extratropical cyclones and is characterized by warm temperatures, weak stratification, large water vapor content, and strong low-altitude winds' [Browning and Pardoe (1973), as referenced in Ralph and others (2005)]. Most studies agree that low-level jets may be found at an altitude of ~1 km, but wind speeds may range from 23 to 35 m s^{-1} (Lackmann, 2002; Ralph and others, 2005). However, in Arctic locations, weaker low-level jets

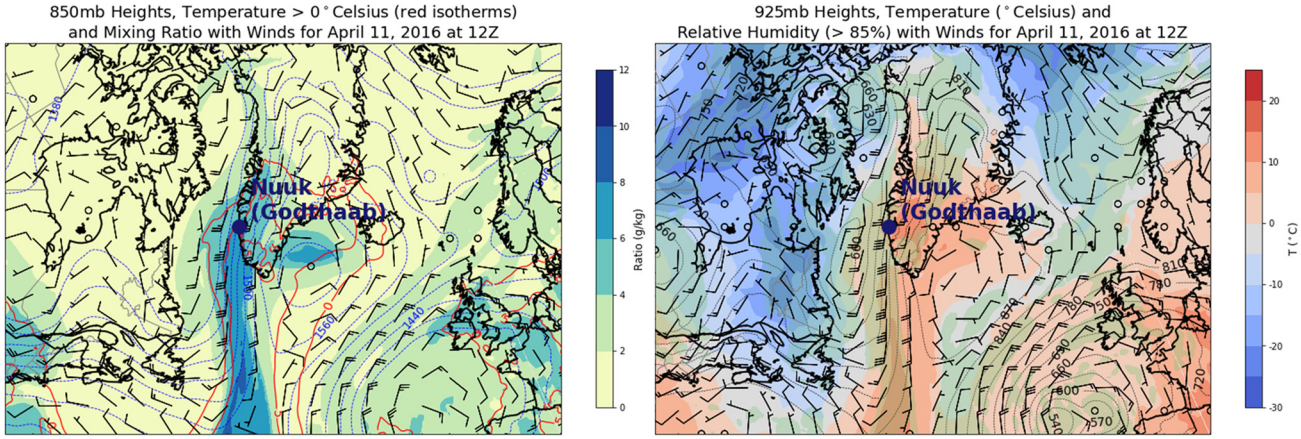

Figure 3. The 2016 Western Greenland case middle to lower atmospheric levels. The 850 mb geopotential heights are plotted on the left (which also includes mixing ratio values, winds and air temperatures above 0°C). The 925 mb heights, winds, air temperatures and relative humidity above 85% (filled green contour) are plotted on the right.

https://doi.org/10.1017/aog.2023.25 Published online by Cambridge University Press

may be just as impactful. For example, an event near Barrow, Alaska, associated with a low-level jet of only 16 m s^{-1} sufficiently warmed and moistened the boundary layer (Intrieri and others, 2014).

While the 850 and 925 mb analyses in Figure 3 show the zones of higher air temperatures and moisture content, they also depict areas of warm air advection, moisture transport and the important low-level jet. These analyses reveal how the low-level jet links to these narrow corridors of enhanced water vapor transport and unusually high air temperatures, with higher wind speeds in line with these zones. The warm air and moisture advection is clearly linked to the largely southerly flow (winds blowing from south to north) across much of southern Greenland. The height equivalent of the 850 mb level ranges from 1000 to 1500 m and from 400 to 800 m at the 925 mb level. Incorporating these levels with these case studies, one should be able to discern a low-level jet from the reanalysis.

The 2016 Greenland ROS case provides an impressive example of a corridor of high air temperatures and a narrow area of elevated moisture associated with a low-level jet. ERA5 fields for 11 April show air temperatures >5°C at 850 mb and as high as 10–15°C across southern Greenland nearer the surface at 925 mb. Figure 4 also shows precipitable water values of 12–16 mm over much of the southwest coast of Greenland, peaking in some locations at 20–24 mm on 11 April. Climatological values of precipitable water in this area on 11 April average between 2 and 7 mm from the southwest coastline and extending inland. Wind speeds reach an impressive 40 m s^{-1} at some locations along the southwest coastline in the low- to mid-levels of the atmosphere. The strong low-level jet, the position of moisture sources (North Atlantic) and the overall blocking setup appear to have worked in combination to produce this ROS event.

An extended area of elevated values of vertically integrated water vapor transport, or IVT, is also captured in Figure 4, with maximum values between 800 and 1000 kg m^{-1} s^{-1} just off the southwest coast of Greenland. Based on previous AR studies, the presence of an IVT contour of 250 kg m^{-1} s^{-1} stretching over 2000 km – usually from a subtropical source south of (or near) 30°N latitude – typically meets the AR classification (Rutz and others, 2014; Ralph and others, 2017; Zhou and others, 2021). Additionally, the Ralph and others (2005) study shows that the combination of strong winds associated with a low-level jet (as evidenced in Fig. 3), as well as the high water vapor content and transport, generally creates an environment suitable for AR initiation. Subsequently, this represents a case where an AR made direct landfall at the location of interest. The AR likely contributed to the increased warm air advection and moisture transport necessary for this ROS event and played a role in the extreme precipitation conditions experienced in southwest Greenland. Comparing Figure 4 to Figure 2, the blocking pattern likely had an influence on this AR setup, allowing for a large enough gradient to form between the ridge and westernmost low-pressure system.

Atmospheric soundings

The sounding for 11 April at 12Z (top panel of Fig. 5) captures the high moisture content and high air temperatures in the lower atmospheric levels with the 2016 Greenland ROS event. Recall that 11 April had the highest recorded wet-snow avalanche activity for this ROS event. Note the strength of the 'warm nose' with this sounding. An air temperature inversion extends from the surface to about the 950 mb level, with air temperatures reaching just above 5°C between the surface and the 900 mb level. This low-level inversion is what gives it the name 'warm nose'. The low-level jet, with winds above 26 m s^{-1} in the middle to low levels of the atmosphere, is one of the more pronounced meteorological features in this case. The strength of the low-level jet (with wind directions largely out of the south, southwest) likely assisted in enhanced warm air advection and moisture transport. In addition, the precipitable water value of 19.58 mm calculated from this sounding is well above average for this time of year.

The lower sounding panel of Figure 5 reveals how the atmospheric profile evolved in the days following the ROS event. This sounding from 16 April (5 d later) is comparatively drier, with a precipitable water of 3.99 mm. A different air mass moved into the region following the passage of a likely cold front and brought much lower temperatures and the drier conditions. Air temperatures are below freezing through the entire atmospheric profile. Also noticeable are the changes in both the wind directions and speeds. Where the low-level jet was prominent in the sounding

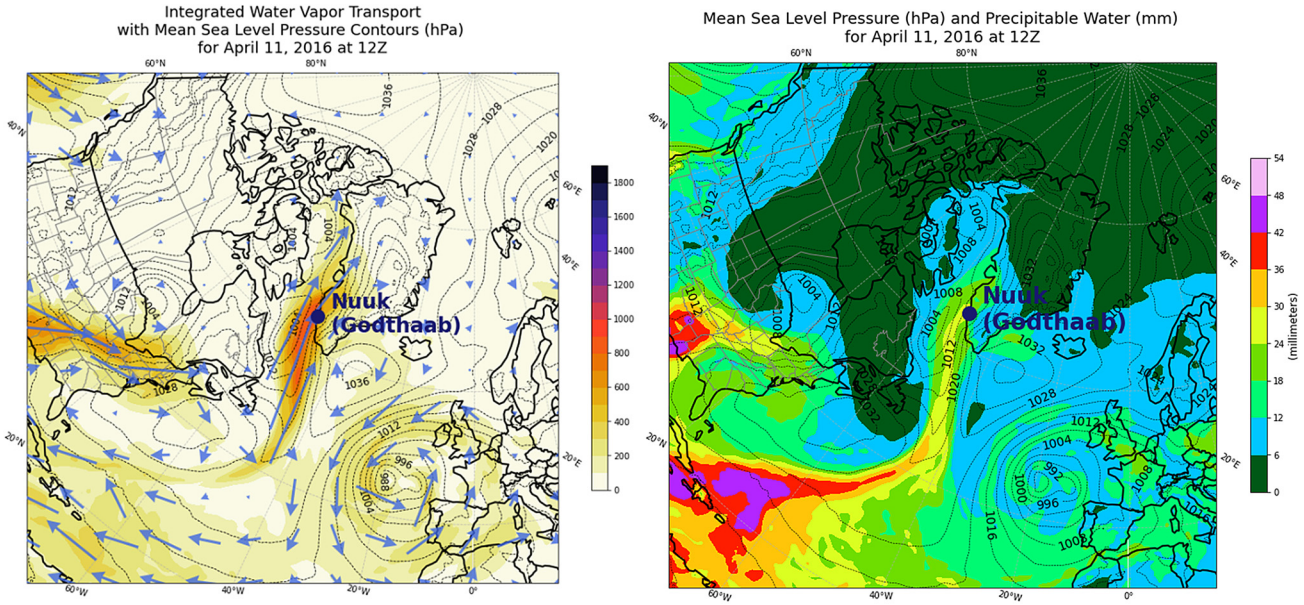

Figure 4. The 2016 Western Greenland case moisture variables. Integrated water vapor transport, with mean sea level pressure as black contours, is plotted on the left, and precipitable water, with similar mean sea level pressure contours, is plotted on the right. The vapor transport visualization includes magnitudes as filled contours, and vector arrows provide the direction.

https://doi.org/10.1017/aog.2023.25 Published online by Cambridge University Press

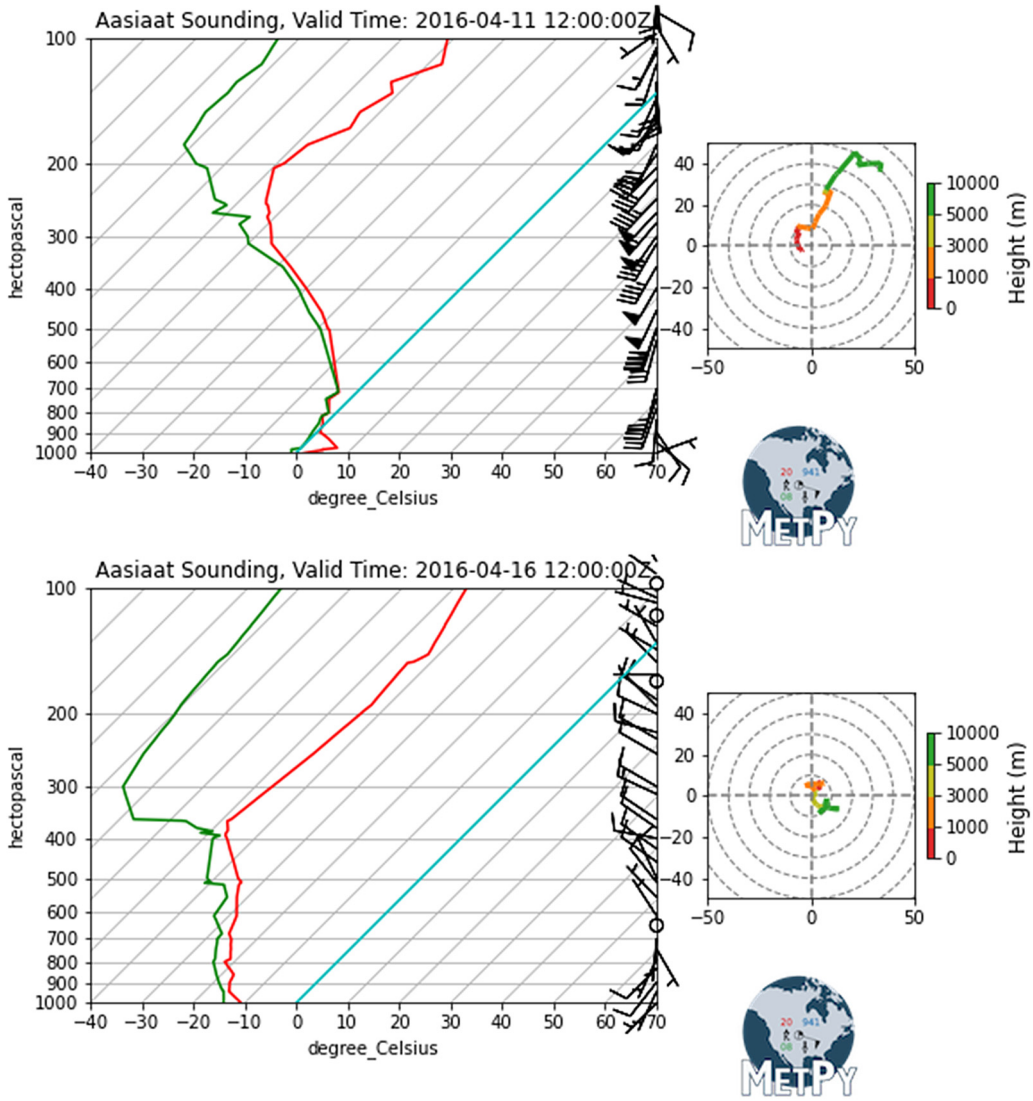

Figure 5. Aasiaat, Greenland (north of Nuuk), during and post rain-on-snow event soundings. The top sounding shows the atmospheric conditions on 11 April 2016. The bottom sounding shows the atmospheric conditions 5 d later. The red and green lines represent air temperature and dewpoint temperature plotted with height, respectively, and winds are plotted as both barbs on the sounding's right and as a hodograph on the right-hand side of the figure.

taken on 11 April, with largely southwesterly winds, the sounding on 16 April shows light wind speeds around 10–15 m s^{-1} throughout the entire column and a northwesterly direction above the mid-levels.

Automatic surface observing stations

Surface observations from the Godthaab station (Fig. 6) revealed a pattern of rising air temperatures prior to the ROS event with a corresponding change to liquid precipitation. Like the Abermann and others (2019) analysis presented earlier, the surface air temperature increased by almost 20°C in a 2 d period from 9 to 11 April, coinciding with a liquid precipitation event. The surface station data showed the temperature rising from −2°C at 1050Z on 9 April to its highest temperature recorded during the period (17°C) at the same time on 11 April, a highly anomalous value for Greenland in April.

Temperatures then decreased in the following days, with air temperatures dropping below freezing beginning on 13 April. Precipitation generally transitioned to solid categories at this point, with one brief period of liquid on 14 April and intervals of mixed precipitation scattered throughout. Air temperatures then remained mostly below freezing following on 15 April. This would have allowed the previous liquid that fell with the initial storm system to freeze on or within the snowpack.

January 2021 Iqaluit, Canada, rain-on-snow event

Atmospheric reanalysis

The Arctic Rain-on-Snow Study team was made aware of ROS conditions occurring in Iqaluit, Canada, on 19 January 2021, through an eyewitness. The weaker Iqaluit ROS case exhibited some similarities with the 2016 Greenland case, as well as notable differences. As seen in the left-hand panel of Figure 7, an upper-level block was present, but it was more representative of a Rex Block or Dipole Block, as opposed to the Omega Block seen in the 2016 Greenland case. Rex Blocks form when a trough undercuts a ridge, so the synoptic pattern appears as a ridge positioned poleward over a trough.

The right-hand panel of Figure 7 shows a strong jet streak at 500 mb (with wind speeds exceeding 55 m s^{-1}) on the equatorward side of a deep trough extending across eastern Canada – likely assisting in maintaining the overall block by undercutting the ridge. Another weaker jet streak (with winds between 30 and 35 m s^{-1}) is located on the western, or left, side of the ridge of high-pressure positioned over southern Greenland. This

https://doi.org/10.1017/aog.2023.25 Published online by Cambridge University Press

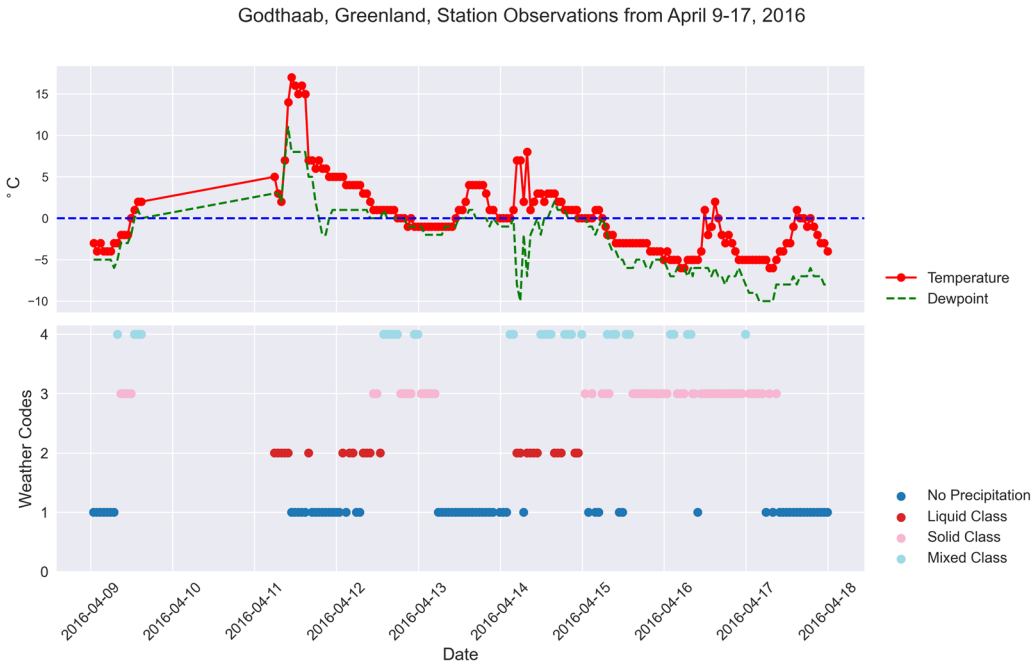

Figure 6. Godthaab (Nuuk), Greenland, surface station observations (9–17 April 2016). Temperature and dewpoint temperature are plotted in the upper panel in °C, and the corresponding precipitation types are plotted in the lower panel.

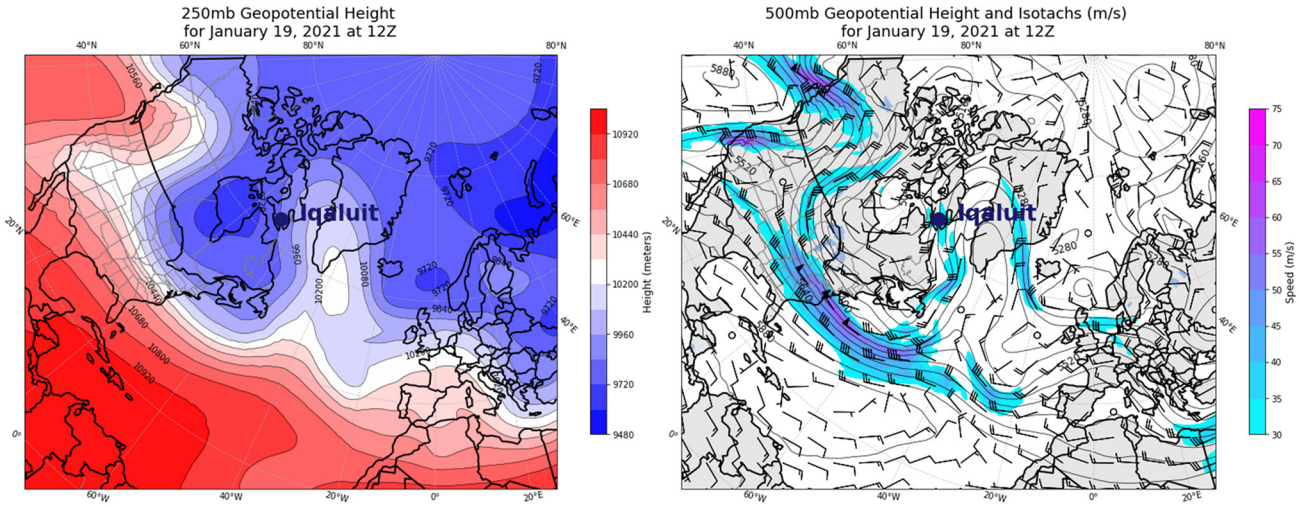

Figure 7. The 2021 Iqaluit case upper atmospheric levels. The 250 mb geopotential heights are plotted on the left, and the 500 mb heights and winds are plotted on the right. The 500 mb panel also includes isotachs (lines of constant wind speed) in m s^{-1} in filled contours, in addition to wind barbs that indicate both direction and speed.

implies additional dynamics influencing precipitation over the southern tip of Baffin Island. Even though the winds in this jet streak were largely from the south, like the Greenland case, speeds were not as strong. However, it did represent another instance of the location of interest positioned directly beneath the southerly flow aloft.

Precipitation produced during the 2021 Iqaluit event, like the 2016 Greenland event, is largely dynamically driven. As with the Greenland event, a shortwave trough (Fig. 7) progressing north toward Baffin Island on 19 January provides the rising motion necessary for precipitation generation. Iqaluit lies in an inlet linked to Frobisher Bay, and the surrounding terrain lies between 500 and 1000 m. Hence, orographic lifting may have also been a contributing factor, as we also surmise for the 2016 Greenland ROS event.

Like the 2016 Greenland ROS case, the 2021 Iqaluit event is linked to narrow corridors of strong moisture transport and warm air advection. However, air temperatures with this case remained just below freezing in the middle to lower levels, and precipitable water values were lower. Figure 8 shows air temperatures at the 925 mb level (right-hand panel) in the 0 to −8°C range over Iqaluit. The only area with air temperatures above freezing at this level is over southern Greenland, which also extends to the 850 mb level (left-hand panel). Mixing ratios are also lower compared to the Greenland case. However, precipitable water values (while modest) are above average, ranging from 8 to 12 mm across the southern tip of Baffin Island (right-hand panel of Fig. 9). Climatological precipitable water values for 19 January span from 1 to 4 mm across southern Baffin Island.

Southerly winds persist throughout the troposphere over Iqaluit, like the Greenland case. The 2021 Iqaluit event also

https://doi.org/10.1017/aog.2023.25 Published online by Cambridge University Press

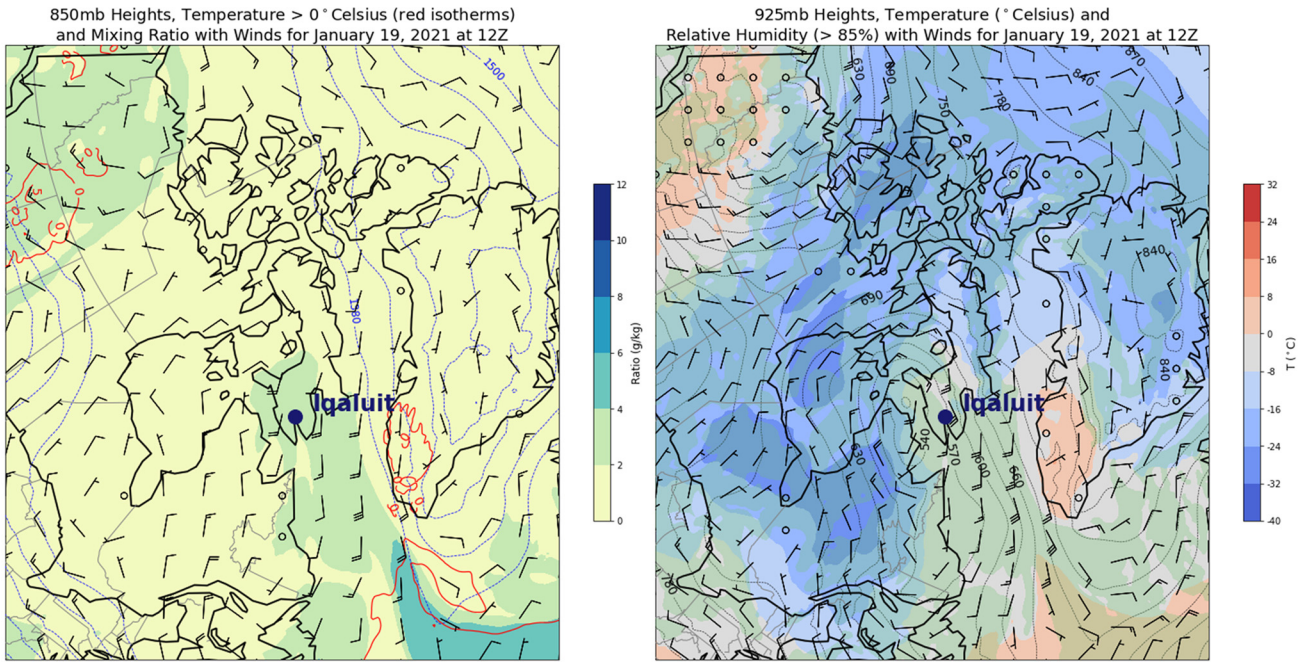

Figure 8. The 2021 Iqaluit case middle to lower atmospheric levels. The 850 mb geopotential heights are plotted on the left (which also includes mixing ratio values, winds and air temperatures above 0°C). 925 mb heights, winds, air temperatures and relative humidity above 85% (filled green contour) are plotted on the right.

exhibits a cyclone-induced low-level jet but with weaker speeds compared to the 2016 Greenland case. Wind speeds are around 20 m s^{-1} in the 850 mb analysis and around 30 m s^{-1} at 925 mb (Fig. 8). These lower-level winds are associated with the warm sector of a cyclone centered near the northern tip of Quebec.

A comparatively large difference with this case is the AR influence. Where the direct impact of a landfalling AR was associated with the ROS event in Greenland, the Iqaluit ROS event appears to have been indirectly influenced by an AR. The same cyclone that produces precipitation in the Iqaluit region likely stripped moisture from the AR present in the North Atlantic as it rounded the broad low-pressure area over eastern Canada (left-hand panel of Fig. 9). The right-hand panel of Figure 9 shows a similar pattern in precipitable water, with higher values (up to 42 mm) reflecting the position of the AR and a narrow corridor of 12–18 mm flowing north toward Baffin Island.

Atmospheric soundings

Atmospheric soundings for the 2021 Iqaluit case also highlight significant differences compared to the Greenland case. As seen in the top panel of Figure 10, the warm layer is very much limited to the surface on 19 January with no prominent 'warm nose'. We also saw this in the earlier 925 mb air temperatures in the reanalysis, with no areas exhibiting above freezing conditions. In an extensive study of relationships between sounding profiles and

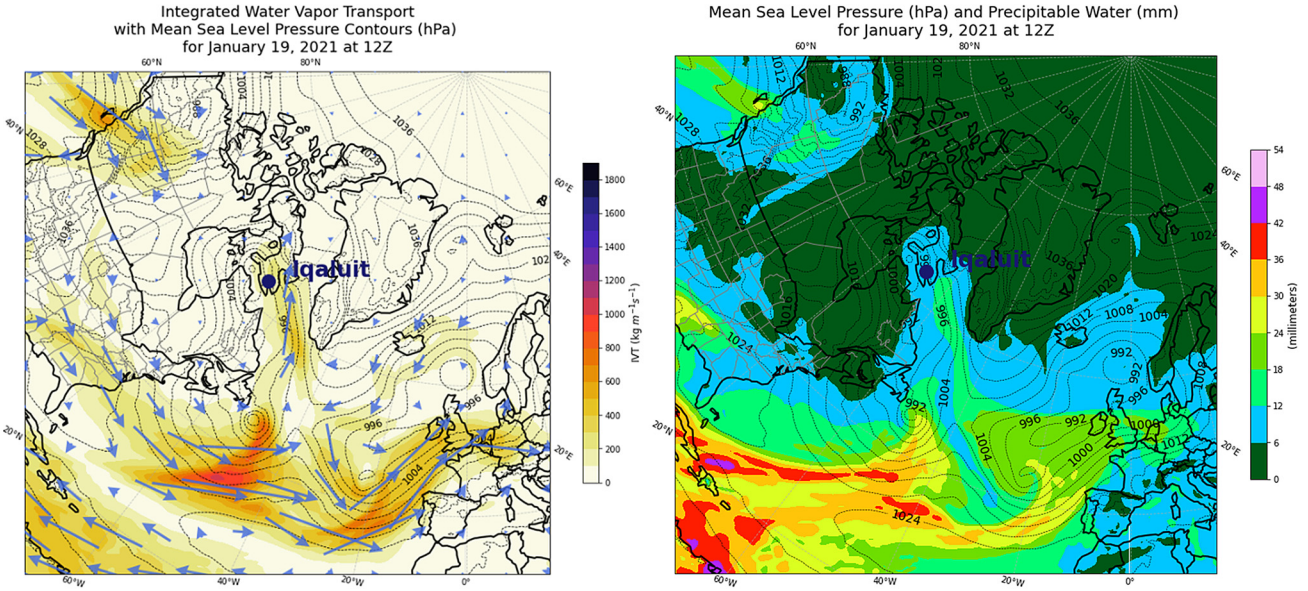

Figure 9. The 2021 Iqaluit case moisture variables. Integrated water vapor transport, with mean sea level pressure as black contours, is plotted on the left, and precipitable water, with similar mean sea level pressure contours, is plotted on the right. The vapor transport visualization includes magnitudes as filled contours, and vector arrows provide the direction.

https://doi.org/10.1017/aog.2023.25 Published online by Cambridge University Press

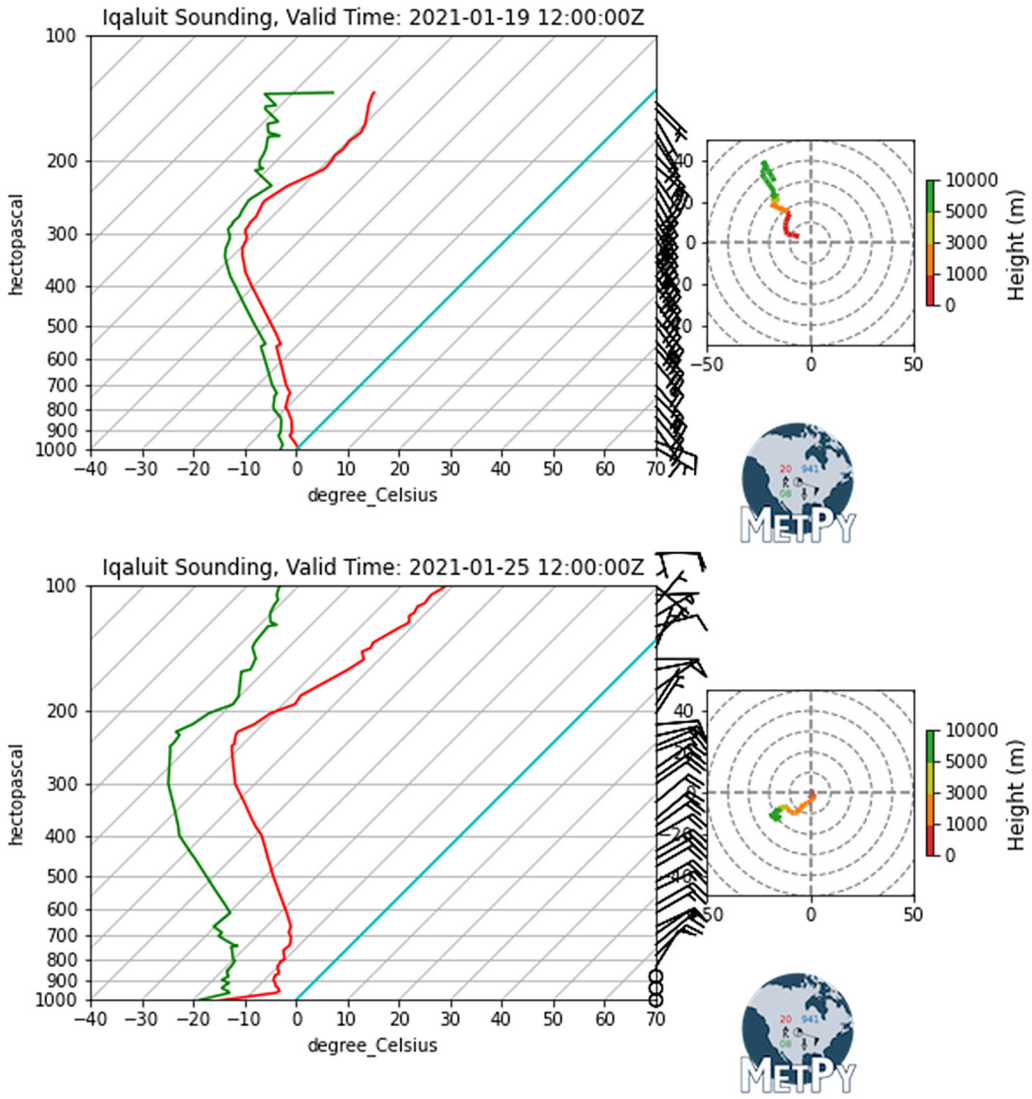

Figure 10. Iqaluit, Nunavut, during and post rain-on-snow event soundings. The top sounding shows the atmospheric conditions on 19 January 2021. The bottom sounding shows the atmospheric conditions 6 d later. The red and green lines represent air temperature and dewpoint temperature plotted with height, respectively, and winds are plotted as both barbs on the sounding's right and as a hodograph on the right-hand side of figure.

precipitation types, Rauber and others (2000) found that for a majority of soundings with no warm layers – such as this example from the Iqaluit case – freezing drizzle was reported.

The Iqaluit sounding from 19 January yields a precipitable water value of 9.19 mm, high for the region and time of year, but modest compared to the 2016 Greenland case. The 19 January sounding also confirms a low-level jet with this case, with wind speeds of 21–26 m s^{-1} between 1 and 2 km above ground level. There is evidence of veering (turning clockwise with height) winds, indicating warm air advection. Direct onshore flow, with winds out of the southeast, is similar to the 2016 Greenland case and provides the additional moisture transport for precipitation.

The sounding for 25 January, 6 d after the ROS event, shows how the atmospheric profile changed when a new air mass moved in and geopotential heights lowered aloft (bottom panel of Fig. 10). Temperatures fell, especially after the passage of the cold front. The moisture profile also became much drier. This sounding's precipitable water fell to 4.28 mm (closer to climatological values) from the 9.19 mm computed from the 19 January sounding. Wind behavior also changed drastically. Wind speeds slackened and directions appeared to back to the northeast, meaning cold air advection.

Automatic surface observing stations

Another interesting aspect of this case is the lack of liquid or even mixed precipitation types recorded in the automated weather station observations at the time of ROS occurrence (Fig. 11). An eyewitness confirmed this ROS event, so this exemplifies a situation where the automated station data (usually collocated with an airport) was not representative of all regional conditions. Rauber and others (2000) noted that soundings yielding deep cloud-top altitudes and no warm layer throughout the atmospheric column (top panel of Fig. 10) may produce a mix of precipitation types, like light snow, ice pellets or freezing rain. Based on data provided by the Moderate Imaging Spectroradiometer instrument aboard the National Aeronautics and Space Administration's Aqua satellite, cloud-top heights in the area were in the range of 4000 to 7000 m during a daytime overpass on 19 January 2021. Rauber and others (2000) noted that some of the soundings in the category exhibiting no warm layers were associated with cloud tops above 5000 m. The authors of that paper also cautioned that surface observations and sounding data are not usually concurrent in place and time. Weather balloons tend to drift downwind from the launch site, especially in strong winds, as was likely the case here.

https://doi.org/10.1017/aog.2023.25 Published online by Cambridge University Press

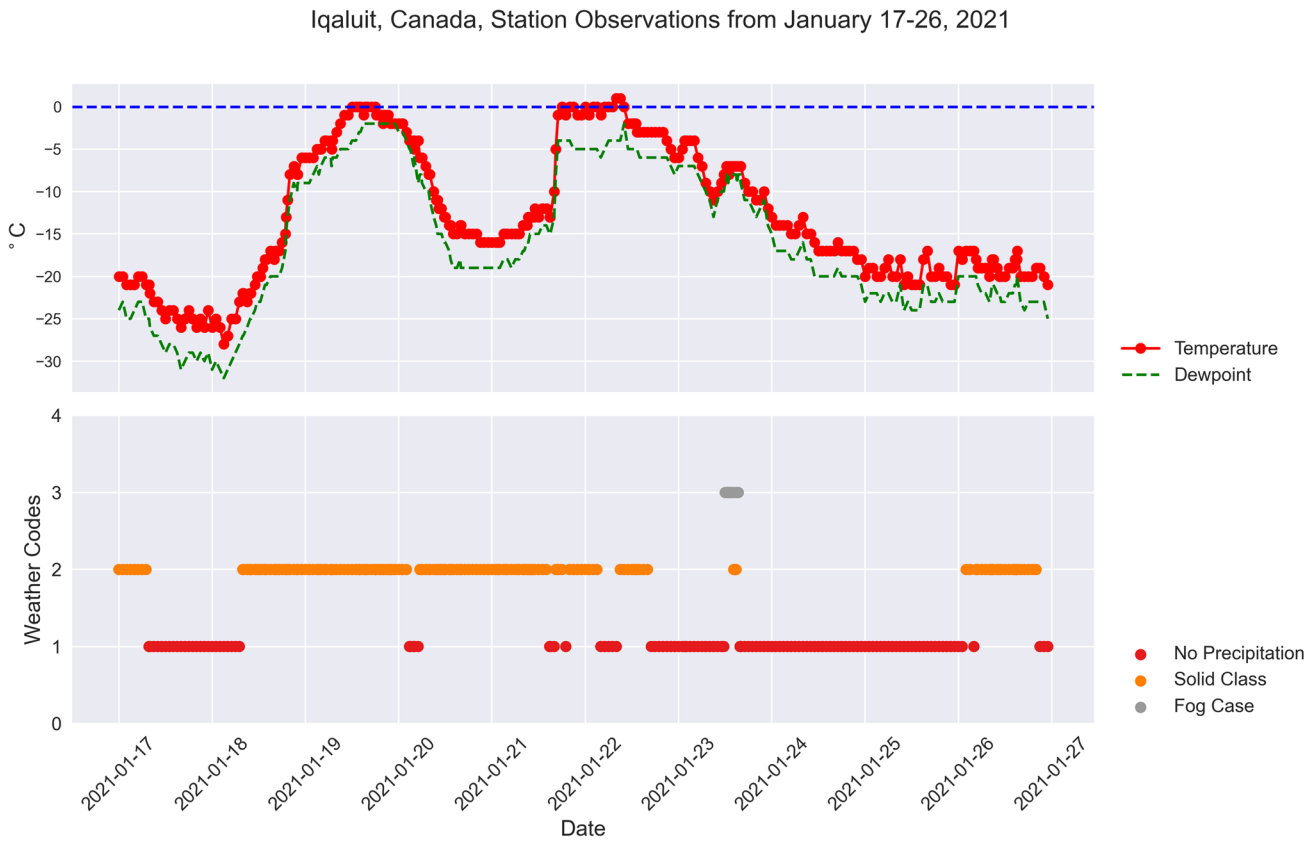

Figure 11. Surface station observations from Iqaluit (17–26 January 2021). Temperature and dewpoint temperature are plotted in the upper panel in °C, and the corresponding precipitation types are plotted in the lower panel.

This was a dynamic weather event, with a relatively strong cyclone, enhanced moisture transport and brisk winds, so it is conceivable that observations may not match actual conditions witnessed in Iqaluit. Nevertheless, the station records demonstrate the same pattern seen with the 2016 Greenland event. Surface air temperatures increased – in this case to just the freezing point on 19 January – with solid precipitation (snow) continuing. Falling air temperatures in successive days would have allowed ice to form from any liquid precipitation that accumulated on the existing snowpack. Surface air temperatures rose to the freezing point again for only a brief period on 22 January but then dropped well below freezing and remained so in the days following.

Summary and concluding thoughts

For the two ROS cases examined here, atmospheric blocking acted as a primary causal mechanism. This reaffirms the importance of blocks, as examined in other ROS cases (Voveris, 2022). With a block, the normal west-to-east geostrophic flow becomes disrupted – replaced by meridional flow – and provides the time for warm air masses to move in and for gradients to build for the additional moisture transport. Blocks may come in a variety of forms, and the differences between the two cases (an Omega Block for the 2016 Greenland event and a Rex Block for the 2021 Iqaluit event) likely led to the difference in strength of ROS conditions. The two sites that experienced ROS were similarly situated directly beneath the strongest southerly flow aloft, between the overall ridge of high-pressure and the westernmost trough of the block. This positioned Iqaluit and Nuuk under an upper-level jet streak, which generated additional jet dynamics for precipitation. Blocking patterns in these cases, and other cases examined by Voveris (2022), developed a few days prior to the day (or days) of ROS conditions and required a few days after the event to weaken and for the geostrophic flow to return to somewhat 'normal' conditions.

Another key component to Arctic ROS formation was the presence of an AR and its direct or indirect influences, which reiterates findings from Voveris (2022). ARs represent a significant source of water vapor transport (and associated high air temperatures) outside of the tropics. When ARs breach the higher latitudes during the winter months, they allow warm, moist conditions to overcome the typical cold, dry Arctic environment and limited solar radiation to produce ROS. We found that the 2016 Greenland ROS event resulted from a direct AR influence (with the AR making landfall), while the 2021 Iqaluit ROS event was influenced indirectly by a cyclone stripping moisture from an AR and carrying this moisture north. The direct AR landfall at Nuuk, Greenland, led to a more pronounced ROS event, and the lack of a direct AR landfall at Iqaluit contributed to lesser ROS-related impacts.

We also revealed the importance of smaller scale atmospheric features, like cyclone-induced low-level jets and 'warm noses' associated with increased moisture transport. Soundings showed how the 2016 Greenland case – directly influenced by an AR – exhibited a strong low-level jet, a deep 'warm nose' layer, and a mostly saturated atmospheric column. Comparatively, the 2021 Iqaluit case was impacted by the same features but to a lesser extent. Moisture and air temperatures were lower, no 'warm nose' was present, and the low-level jet was weaker, a possible consequence of only the indirect influence of an AR. These combined features were enough to adequately warm and moisten the boundary layer, leading to the report of ROS in Iqaluit, but were not enough to produce a strong ROS event as seen at Nuuk, Greenland.

To our knowledge, our study is the first to show how atmospheric blocking, ARs and other mesoscale features, such

https://doi.org/10.1017/aog.2023.25 Published online by Cambridge University Press

as low-level jets and subsequent 'warm noses', work in tandem to produce Arctic ROS events of differing magnitudes. In a recent study by Serreze and others (2022), the key meteorological features discussed here, and noted by Voveris (2022) for other ROS events, can also be associated with Arctic precipitation events of extreme magnitude (either snow- or rain-driven). The interplay between these meteorological drivers is complex and will vary on a case-by-case basis, but some connections have been established between these features themselves and the influence they have on precipitation generation. For example, Ralph and others (2005) note that low-level jets may coincide with AR development when combined with high water vapor content and transport. A study from Benedict and others (2019) demonstrates how atmospheric blocking slows the normal progression of shortwave systems, shifting the storm track equatorward, while the high-pressure ridge (resulting from the blocking and developing 7–10 days prior to an AR) directs more systems toward the study area. This leads to higher chances of both AR incidence and extreme precipitation events (Benedict and others, 2019).

Having established these meteorological links to Arctic ROS events, we can infer how future global warming might influence ROS occurrence and intensity. Uncertainties remain regarding how climate change will affect atmospheric blocking. Some studies argue that blocking patterns might decrease in frequency in the middle latitudes as the climate warms or that areas that experience a climatologically high number of blocking episodes may see a shift in those areas (Woollings and others, 2018). However, Woollings and others (2018) caution that the ability of climate models to handle blocks remains unclear and that natural variability is likely to have a strong influence on blocking patterns in coming decades. They also add that the effect of wintertime blocking on air temperatures is dependent upon thermal advection – a process expected to weaken in a warming world – but the effect of summertime blocking on air temperatures may strengthen from feedbacks resulting from changes in soil moisture.

Results from climate model studies are in general agreement that future warming will coincide with increased poleward moisture transport and elevated Arctic precipitation with a transition to a more rain-dominated climate (Lenaerts and others, 2020; McCrystall and others, 2021; Niwano and others, 2021). More rainfall implies more ROS events. However, a shorter snow cover season may lead to fewer ROS events, especially during the autumn or spring months, or to more incidents of rain falling on frozen ground instead. In addition, Espinoza and others (2018) found that climate models project a 10% decrease in the number of ARs, based on the 'worst-case' global emissions scenario from the Intergovernmental Panel on Climate Change. However, they note that models also project ARs to be 25% longer, 25% wider and have larger IVT values, likely due to the increasing moisture available in a warming atmosphere. This implies that more ARs may potentially reach high Arctic regions, and stronger IVT may lead to more extreme precipitation events coinciding with ROS conditions.

Acknowledgements. This study was supported by the National Science Foundation Grant ICER 1928230 'NNA Track 1: A Systematic Pan-Arctic Analysis of Rain on Snow and Extreme Precipitation Events and their Impacts on Human-Environment Systems'. We thank Mistia Zuckerman and Tori McLeod for their time and effort in the final editing and submission of this manuscript. We also appreciate the ECMWF and UCAR for their data and MetPy programming codes (respectively) used in this research. We accessed ERA5 data from the Copernicus Climate Data Store API [Application Program Interface], maintained by the ECMWF.

References

Abermann J, Eckerstorfer M, Malnes E and Ulf Hansen B (2019) A large wet snow avalanche cycle in west Greenland quantified using remote sensing and in situ observations. *Natural Hazards* **97**(2), 517–534. doi: 10.1007/s11069-019-03655-8

Benedict JJ, Clement AC and Medeiros B (2019) Atmospheric blocking and other large-scale precursor patterns of landfalling atmospheric rivers in the North Pacific: a CESM2 study. *Journal of Geophysical Research: Atmospheres* **124**(21), 11330–11353. doi: 10.1029/2019JD030790

Bieniek P and 6 others (2018) Assessment of Alaska rain-on-snow events using dynamical downscaling. *Journal of Applied Meteorology and Climatology* **57**(8), 1847–1863. doi: 10.1175/JAMC-D-17-0276.1

CBC News (2021) Iqaluit sets record high temperature for 19 January, reaching 0.5 C. CBC News. CBC. https://www.cbc.ca/news/canada/north/iqaluit-sets-record-high-temperature-for-jan-19-reaching-0-5-c-1.5882621

Cohen J and 6 others (2014) Recent arctic amplification and extreme mid-latitude weather. *Nature Geoscience* **7**(9), 627–637. doi: 10.1038/ngeo2234

Cohen J, Ye H and Jones J (2015) Trends and variability in rain-on-snow events. *Geophysical Research Letters* **42**(17), 7115–7122. doi: 10.1002/2015GL065320

Crawford AD, Alley KE, Cooke AM and Serreze MC (2020) Synoptic climatology of rain-on-snow events in Alaska. *Monthly Weather Review* **148**(3), 1275–1295. doi: 10.1175/MWR-D-19-0311.1

Espinoza V, Waliser DE, Guan B, Lavers DA and Ralph FM (2018) Global analysis of climate change projection effects on atmospheric rivers. *Geophysical Research Letters* **45**(9), 4299–4308. doi: 10.1029/2017GL076968

Forbes BC and 6 others (2016) Sea ice, rain-on-snow and tundra reindeer nomadism in Arctic Russia. *Biology Letters* **12**(11), 20160466. doi: 10.1098/rsbl.2016.0466

Garvelmann J, Pohl S and Weiler M (2015) Spatio-temporal controls of snowmelt and runoff generation during rain-on-snow events in a mid-latitude mountain catchment. *Hydrological Processes* **29**(17), 3649–3664. doi: 10.1002/hyp.10460

Graham RM, Hudson SR and Maturilli M (2019) Improved performance of ERA5 in Arctic gateway relative to four global atmospheric reanalyses. *Geophysical Research Letters* **46**(11), 6138–6147. doi: 10.1029/2019GL082781

Grenfell TC and Putkonen J (2008) A method for the detection of the severe rain-on-snow event on banks island, October 2003, using passive microwave remote sensing. *Water Resources Research* **44**(3), W03425. doi: 10.1029/2007WR005929

Guan B, Waliser DE, Ralph FM, Fetzer EJ and Neiman PJ (2016) Hydrometeorological characteristics of rain-on-snow events associated with atmospheric rivers. *Geophysical Research Letters* **43**(6), 2964–2973. doi: 10.1002/2016GL067978

Hansen BB and 8 others (2014) Warmer and wetter winters: characteristics and implications of an extreme weather event in the high Arctic. *Environmental Research Letters* **9**(11), 114021. doi: 10.1088/1748-9326/9/11/114021

Hersbach H and 6 others (2020) The ERA5 global reanalysis. *Quarterly Journal of the Royal Meteorological Society* **146**(730), 1999–2049. doi: 10.1002/qj.3803

Hoffmann L and 10 others (2019) From ERA-Interim to ERA5: the considerable impact of ECMWF's next-generation reanalysis on Lagrangian transport simulations. *Atmospheric Chemistry and Physics* **19**, 3097–3124. doi: 10.5194/acp-19-3097-2019

Intrieri JM and 8 others (2014) Global Hawk Dropsonde observations of the Arctic atmosphere obtained during the Winter Storms and Pacific Atmospheric Rivers (WISPAR) field campaign. *Atmospheric Measurement Techniques* **7**(11), 3917–3926. doi: 10.5194/amt-7-3917-2014

Kattelmann RC (1997) Flooding from rain-on-snow events in the Sierra Nevada. *Destructive Water: Water-Caused Natural Disasters, Their Abatement and Control*. International Association of Hydrological Sciences.

Lackmann GM (2002) Cold-frontal potential vorticity maxima, the low-level jet, and moisture transport in extratropical cyclones. *Monthly Weather Review* **130**(1), 59–74. doi: 10.1175/1520-0493(2002)130<0059:CFPVMT>2.0.CO;2

Lenaerts JTM, Camron MD, Wyburn-Powell CR and Kay JE (2020) Present-day and future Greenland Ice Sheet precipitation frequency from CloudSat observations and the Community Earth System Model. *The Cryosphere* **14**(7), 2253–2265. doi: 10.5194/tc-14-2253-202

McCabe GJ, Clark MP and Hay LE (2007) Rain-on-snow events in the western United States. *Bulletin of the American Meteorological Society* **88**(3), 319–328. doi: 10.1175/BAMS-88-3-319

McCrystall MR, Stroeve J, Serreze M, Forbes BC and Screen JA (2021) New climate models reveal faster and larger increases in Arctic precipitation than previously projected. *Nature Communications* **12**(1), 6765. doi: 10.1038/s41467-021-27031-y

Niwano M and 5 others (2021) Rainfall on the Greenland ice sheet: present-day climatology from a high-resolution non-hydrostatic polar regional climate model. *Geophysical Research Letters* **48**(15), e2021GL092942. doi: 10.1029/2021GL092942

Nunatsiaq News (2021) Mild stretch sets the stage for record-breaking warmth in Iqaluit. *Nunatsiaq News*. https://nunatsiaq.com/stories/article/mild-stretch-sets-the-stage-for-record-breaking-warmth-in-iqaluit/

Pan CG, Kirchner PB, Kimball JS, Kim Y and Du J (2018) Rain-on-snow events in Alaska, their frequency and distribution from satellite observations. *Environmental Research Letters* **13**(7), 075004. doi: 10.1088/1748-9326/aac9d3

Putkonen J and Roe G (2003) Rain-on-snow events impact soil temperatures and affect ungulate survival. *Geophysical Research Letters* **30**(4). doi: 10.1029/2002GL016326

Ralph FM and 6 others (2017) Atmospheric rivers emerge as a global science and applications focus. *Bulletin of the American Meteorological Society* **98** (9), 1969–1973. doi: 10.1175/BAMS-D-16-0262.1

Ralph FM, Neiman PJ and Rotunno R (2005) Dropsonde observations in low-level jets over the northeastern Pacific Ocean from CALJET-1998 and PACJET-2001: mean vertical-profile and atmospheric-river characteristics. *Monthly Weather Review* **133**(4), 889–910. doi: 10.1175/MWR2896.1

Rauber RM, Olthoff LS, Ramamurthy MK and Kunkel KE (2000) The relative importance of warm rain and melting processes in freezing precipitation events. *Journal of Applied Meteorology and Climatology* **39**(7), 1185–1195. doi: 10.1175/1520-0450(2000)039<1185:TRIOWR>2.0.CO;2

Rennert KJ, Roe G, Putkonen J and Bitz CM. (2009) Soil thermal and ecological impacts of rain on snow events in the circumpolar Arctic. *Journal of Climate* **22**(9), 2302–2315. doi: 10.1175/2008JCLI2117.1

Rutz JJ, Steenburgh WJ and Ralph FM (2014) Climatological characteristics of atmospheric rivers and their inland penetration over the Western United States. *Monthly Weather Review* **142**(2), 905–921. doi: 10.1175/MWR-D-13-00168.1

Semmens KA, Ramage J, Bartsch A and Liston GE (2013) Early snowmelt events: detection, distribution, and significance in a major sub-Arctic watershed. **8**(1), 014020. doi: 10.1088/1748-9326/8/1/014020

Serreze MC and others (2021) Arctic rain on snow events: bridging observations to understand environmental and livelihood impacts. *Environmental Research Letters* **16**(10), 105009. doi: 10.1088/1748-9326/ac269b

Serreze MC and 5 others (2022) Characteristics of extreme daily precipitation events over the Canadian Arctic. *International Journal of Climatology* **42**, 10353–10372. doi: 10.0002/joc.7907

Serreze MC, Crawford AD and Barrett AP (2015) Extreme daily precipitation events at Spitsbergen, an Arctic Island. *International Journal of Climatology* **35**(15), 4574–4588. doi: 10.1002/joc.4308

Singh P, Spitzbart G, Hübl H and Weinmeister HW (1997) Hydrological response of snowpack under rain-on-snow events: a field study. *Journal of Hydrology* **202**(1), 1–20. doi: 10.1016/S0022-1694(97)00004-8

Trubilowicz JW and Moore RD (2017) Quantifying the role of the snowpack in generating water available for run-off during rain-on-snow events from snow pillow records. *Hydrological Processes* **31**(23), 4136–4150. doi: 10.1002/hyp.11310

Voveris JJ (2022) Meteorological drivers of Arctic rain-on-snow events and how climate change may influence associated risks (Order No. 29069573). Available from Dissertations & Theses @ University of Colorado, Boulder; Dissertations & Theses @ University of Colorado System; ProQuest Dissertations & Theses A&I; ProQuest Dissertations & Theses Global. (2681751208). Retrieved from https://colorado.idm.oclc.org/login.

Woollings T and 8 others (2018) Blocking and its response to climate change. *Current Climate Change Reports* **4**(3), 287–300. doi: 10.1007/s40641-018-0108-z

Zhou Y and 5 others (2021) Uncertainties in atmospheric river lifecycles by detection algorithms: climatology and variability. *Journal of Geophysical Research: Atmospheres* **126**(8), e2020JD033711. doi: 10.1029/2020JD033711

https://doi.org/10.1017/aog.2023.25 Published online by Cambridge University Press